Modeling near-field tsunami observations to improve finite-fault slip models for the 11 March 2011 Tohoku earthquake

Y. Yamazaki,[1] T. Lay,[2] K. F. Cheung,[1] H. Yue,[2] and H. Kanamori[3]

Received 1 August 2011; revised 15 September 2011; accepted 16 September 2011; published 18 October 2011.

[1] The massive tsunami generated by the 11 March 2011 Tohoku earthquake (M_w 9.0) was widely recorded by GPS buoys, wave gauges, and ocean bottom pressure sensors around the source. Numerous inversions for finite-fault slip time histories have been performed using seismic and/or geodetic observations, yielding generally consistent patterns of large co-seismic slip offshore near the hypocenter and/or up-dip near the trench, where estimated peak slip is ~60 m. Modeling the tsunami generation and near-field wave processes using two detailed rupture models obtained from either teleseismic P waves or high-rate GPS recordings in Japan allows evaluation of how well the finite-fault models account for the regional tsunami data. By determining sensitivity of the tsunami calculations to rupture model features, we determine model modifications that improve the fit to the diverse tsunami data while retaining the fit to the seismic and geodetic observations. **Citation:** Yamazaki, Y., T. Lay, K. F. Cheung, H. Yue, and H. Kanamori (2011), Modeling near-field tsunami observations to improve finite-fault slip models for the 11 March 2011 Tohoku earthquake, *Geophys. Res. Lett.*, *38*, L00G15, doi:10.1029/2011GL049130.

1. Introduction

[2] The great 11 March 2011 Tohoku earthquake (M_w 9.0) produced unprecedented geophysical data sets of global and regional seismic observations, continuously recorded GPS ground motions, deep water and coastal tsunami recordings, and ocean bottom displacement and tsunami run-up measurements. Working toward integrated models of the rupture process that can account for the diverse observations is a major undertaking.

[3] Many characterizations of the rupture process have already been produced by analyses of different data types, including teleseismic and regional body and surface waves recordings [e.g., *Ammon et al.*, 2011; *Hayes*, 2011; *Ide et al.*, 2011; *Koper et al.*, 2011; *Lay et al.*, 2011b; *Shao et al.*, 2011; *Simons et al.*, 2011; *Yoshida et al.*, 2011], GPS observations [e.g., *Iinuma et al.*, 2011; *Ito et al.*, 2011; *Ozawa et al.*, 2011; *Simons et al.*, 2011; *Yue and Lay*, 2011], and tsunami recordings [e.g., *Lay et al.*, 2011a; *Fujii et al.*, 2011; *Hayashi et al.*, 2011; *Maeda et al.*, 2011; *Simons et al.*, 2011]. There is general consistency amongst these models in terms of primary fault displacements being located in the up-dip portion of the megathrust, and lower amounts of slip but stronger short-period seismic wave radiation in the down-dip region below the Honshu coastline. However, the models vary substantially in detail due to many factors including model parameterization, data selection, and intrinsic resolution of the various data types. For example, geodetic inversions using only land-based static ground motion observations tend to put less slip near the trench than indicated in some seismic and tsunami models.

[4] Ideally, one would simply combine all observations into joint inversions, but pursuing such an approach is complicated by issues of varying resolution and sensitivity of different data to distinct aspects of the rupture process. While seismic and geodetic inversions for finite-fault models of large earthquakes tend to be highly parameterized and very detailed (albeit, not always consistent), inversions of tsunami observations tend to be simpler in parameterization and lower in resolution due to the long-period nature of the waves [e.g., *Fujii et al.*, 2011; *Maeda et al.*, 2011]. Recognizing the great value of tsunami observations as the lowest velocity waves available for studying large submarine earthquake sources, we take an intermediate approach by computing tsunami waves for detailed rupture models and comparing them to near-field observations for model evaluation. Exploring by forward modeling sensitivity of poorly constrained aspects of the models can improve the fit to the tsunami observations and refine the rupture process obtained through inversion of seismic and geodetic data.

2. Rupture Models and Tsunami Modeling

[5] Of the numerous finite-fault models for the 11 March 2011 Tohoku earthquake, we began our analysis with two representative inversions using seismic and geodetic observations. These are an inversion of teleseismic P waves only (P-MOD2) by *Lay et al.* [2011b] and an inversion of complete high-rate (1 sps) GPS signals from stations in Japan (hrGPS) by *Yue and Lay* [2011]. The two models have similar parameterizations and comprise 20 × 20 km^2 subfaults with fault strike $\varphi_f = 202°$, dip $\delta = 10°$ (increasing to 22° below 27 km depth for the hrGPS model), variable rake for each subfault, and subfault source time functions parameterized by 6-7 overlapping triangular subevents for total possible durations of 32 s (P-MOD2) and 70 s (hrGPS). The two models use the same epicenter (38.107°N, 142.916°E) and origin time 14:46:18.14 UTC from *Zhao et al.* [2011]. The hypocentral depth h = 20 km for P-MOD2 and 22.5 km for hrGPS includes a 3 km deep ocean layer. The rupture front expands over the fault at 1.5 km/s out to a distance of 100 km and then at 2.5 km/s beyond that for both models, based on extensive

[1]Department of Ocean and Resource Engineering, University of Hawaii at Manoa, Honolulu, Hawaii, USA.
[2]Department of Earth and Planetary Sciences, University of California, Santa Cruz, California, USA.
[3]Seismological Laboratory, California Institute of Technology, Pasadena, California, USA.

0094-8276/11/2011GL049130

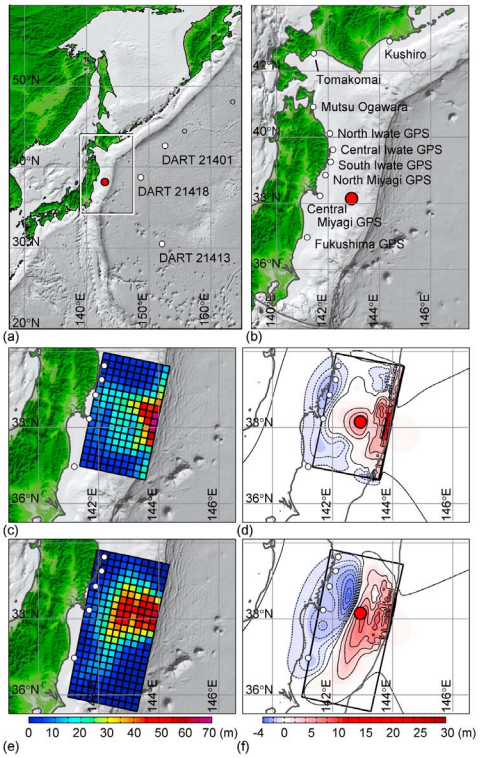

Figure 1. Model setting and data. (a) Level-1 grid and DART buoy locations. (b) Level-2 grid and locations of regional GPS and wave gauges. (c) Slip distribution of P-MOD3. (d) Vertical seafloor displacement for P-MOD3. (e) Slip distribution of hrGPS-2. (f) Vertical seafloor displacement for hrGPS-2.

modeling in the original studies. These finite-fault models are totally independent in terms of input data and have very different degrees of spatial and temporal resolution; hrGPS has better spatial and total seismic moment resolution because it fits all seismic and geodetic motions at 43 regional GPS stations for periods longer than 25 s, while P-MOD2 provides good rupture timing information because it fits teleseismic P waves with periods longer than about 5 s for which the Green functions are very simple.

[6] The tsunami observations available for the 11 March 2011 Tohoku earthquake are the most extensive ever made for a great earthquake. We consider tsunami observations at 6 NOWPHAS GPS buoys, 3 NOWPHAS wave gauges, and 3 NOAA DART stations surrounding the tsunami source as shown in Figures 1a and 1b. These stations recorded the near-field tsunami characteristics, which reflect the subtleties of the source parameters that enable a sensitivity analysis of the two finite fault models. We compute water surface elevations using the non-linear dispersive wave model NEOWAVE (Non-hydrostatic Evolution of Ocean Wave) [*Yamazaki et al.*, 2009, 2011]. The staggered-grid finite difference model includes a vertical momentum equation and a non-hydrostatic pressure term in the nonlinear shallow-water equations to describe tsunami generation from seafloor deformation and propagation of weakly dispersive tsunami waves. The rupture models provide the finite-fault slip time histories to prescribe kinematic seafloor deformation with the planar fault model of *Okada* [1985] for the input to NEOWAVE. Figures 1a and 1b show the level-1 and 2 nested computational domains, which describe propagation of the tsunami across the northwest Pacific at 2 arc-min (~3000 m) resolution, while resolving the finite-fault models, large-scale coastal features, and near-field tsunami waves at 24 arc-sec (~600 m). The bathymetry is derived from the 1 arc min (~1500 m) ETOPO1 data and the 20 arc sec (~475 m) data from the Japan Meteorological Agency (JMA). The latter was derived from nautical charts of the Japan Hydrographic Association and the 500-m J-EGG500 bathymetry data of the Japan Oceanographic Data Center.

3. Model Perturbations and Tsunami Predictions

[7] Our procedure involved calculation of tsunami signals at the available near-field stations, comparison with the records, perturbation of poorly-constrained fault model parameters, re-inversion of the seismic and hrGPS observations, and iteration on forward modeling to gain understanding of what aspects of the two finite-fault models influence the regional tsunami characteristics. We explore perturbations of fault strike, dip, and hypocentral depth, as well as overall dimensions, and inversion smoothing about the P-MOD2 and hrGPS model parameters. Prior analysis supports the seaward concentration of slip found in both finite-fault models, but the parameters listed above are not all well constrained by the seismic and geodetic data [*Lay et al.*, 2011a]. For example, φ_f can vary by 15–20°, δ by about 5°, and h by about 5 km without significantly degrading inversions of the seismic and geodetic data. Smoothing is not well-constrained for finite-fault inversions and absolute slip values in the models are directly influenced by choice of smoothing parameters. The signals for the Tohoku event are dominated by energy from a spatially concentrated main slip patch, with later rupture being less well resolved, so overall fault dimensions are also not tightly constrained.

[8] The sensitivity analysis includes a total of 55 perturbations on the two initial finite-fault models. The preferred perturbed versions of the two models, labeled as P-MOD3 and hrGPS-2, are shown in Figures 1c and 1e with their respective seafloor static vertical motions in Figures 1d and 1f. In both cases, $\varphi_f = 192°$ represents a 10° decrease relative to the initial models. For P-MOD3, $\delta = 12°$ is 2° steeper, the depth below seafloor is increased by 2.5 km, and smoothing is reduced such that slip values average about 10% more in relation to P-MOD2. The fault length is reduced from 380 to 340 km. For hrGPS-2, the cutoff period of the lowpass filter applied to the data is shifted from 25 s to 15 s. These minor perturbations, obtained by forward modeling searches over the parameter space, improve fits to the near-field tsunami observations, with the corresponding inversions to the P waves and hrGPS data literally unchanged. This reflects the fact that the original models provide reasonable fits to the near-field tsunami signals and the efficacy of forward modeling in fine tuning rupture models that are already optimized with seismic and geodetic records.

[9] Formal uncertainties on the model parameters are elusive given the many modeling approximations, trade-offs, and covariance of parameters, but within the class of models considered, we estimate that average δ to be within the 2–3° range from 10° and average φ_f is resolved to within

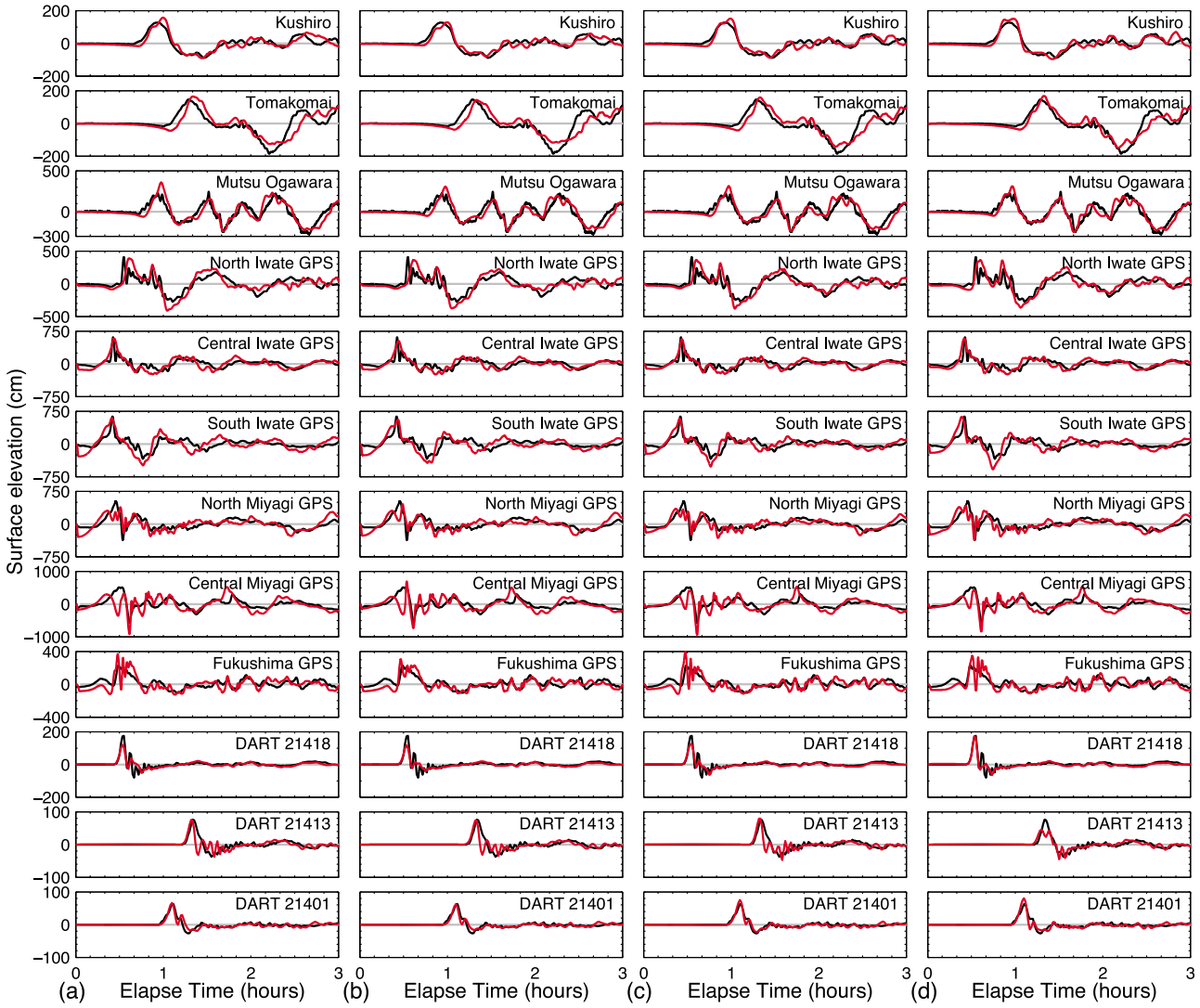

Figure 2. Sensitivity tests of hypocentral depth (h), dip angle (δ), and strike angle (ϕ_f) with 380 km × 200 km fault. Observed (black lines) and the computed (red lines) at water level stations. (a) h = 20 km, δ = 10°, and φ_f = 202°; (b) h = 22.5 km, δ = 10°, and φ_f = 202°; (c) h = 22.5 km, δ = 12°, and φ_f = 202°; (d) h = 22.5 km, δ = 12°, and φ_f = 192°.

the 10° range from 192–202°. Figure 2 provides a sample of the sensitivity tests on the depth and the dip and strike angles with the 380 km × 200 km fault of the P-MOD2 model. The comparison focuses on the initial waveform, which closely relates to the source characteristics. The original P-MOD2 with φ_f = 202° in Figure 2a reproduces the peak at the central and south Iwate GPS buoys as well as DART 21413 and 21401 and captures the first wave at the Fukushima GPS buoy, while showing late arrivals at the Kushiro, Tomakomai, and Mutsu Ogawara wave gauges to the north and underestimating the amplitude at DART 21418. A slight increase in the hypocentral depth and average fault dip shows minor effects in Figures 2b and 2c. Rotation of the strike angle to φ_f = 192° in Figure 2d improves the arrival time at Kushito, Tomakomai, and North Iwate buoys as well as the peak amplitude at the south Iwate GPS and DART 21418 at the expense of the agreement at DART 21413.

[10] Extending the P-MOD2 model 20 km north and removing 60 km from the south improve the arrival time at the northern buoys and prevent late, poorly constrained slip at very shallow depth from generating short-period signals at the Fukushima GPS buoy and the adjacent DART 21413. This leads to the 340 km × 200 km P-MOD3 class of fault models. Figure 3 illustrates their variability in near-field tsunami signals over the range φ_f = 202° to 187°. The models show reduction of the short period waves at the southern buoys, but eliminate the small initial wave at the Fukushima GPS as a trade-off. Among the P-MOD3 class, the model with φ_f = 192° provides our favored solution shown in Figure 4. The computed results provide excellent agreement with the record data including the amplitude at DART 21418 that is sensitive to the strike angle as shown in Figure 3. The fits are comparable to or better than those obtained by direct inversion of tsunami arrivals [e.g., *Fujii et al.*, 2011; *Maeda et al.*, 2011], while the model also represents a least-squares fit to the teleseismic P waves. For the stations near the epicenter, static motions of the seafloor beneath the gauges produce baseline variations, and these are adequately,

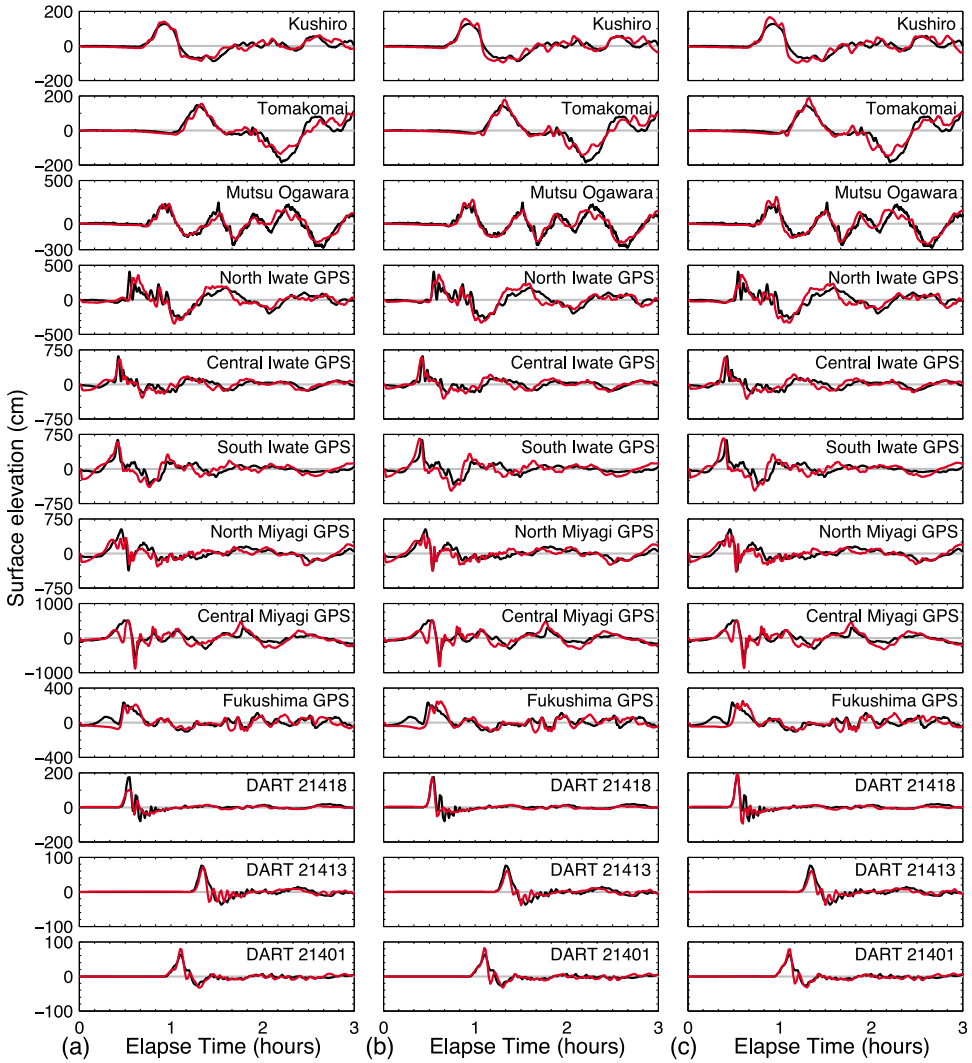

Figure 3. Sensitivity tests of strike angle for P-MOD3 type models (δ = 12°, h = 22.5 km). Observed (black lines) and the computed (red lines) at water level stations. (a) φ_f = 202°. (b) φ_f = 197°. (c) φ_f =187°.

although not perfectly matched by the model. In part this may reflect neglect of surface wave generated tsunami signals, which are expected to be early, relatively short-period features. The computed waveforms reproduce the sharp upward pulse of ~6 m at the central and south Iwate stations that originates from the concentrated slip of up to 70 m in the shallowest portion of the P-MOD3 model near the trench.

[11] We also performed a series of perturbations on the original hrGPS model of *Yue and Lay* [2011]. The upward pulse at the Iwate GPS buoys is not well-matched by any of the hrGPS models that we explored, including the case shown in Figure 5, which is for φ_f = 192°, chosen to match the P-MOD3 favored solution. This model, hrGPS-2, also used less aggressive low pass filtering allowing signals up to 15 s to be modeled in an effort to resolve the localized slip needed to generate the pulse at the Iwate buoys. The intrinsic nature of the hrGPS inversion tends to spread slip over somewhat broader regions of the fault plane, as seen in Figure 1, and this prevents imaging of the concentrated seafloor uplift required to generate the pulse. Other than that, basic features of the regional tsunami signals are adequately matched, although the fits are not as good as for P-MOD3.

4. Discussion and Conclusions

[12] The sensitivity analysis demonstrates the advantage of using tsunami measurements to fine tune finite fault models that are already optimized with seismic and geodetic data. By searching over model parameters that are poorly constrained in finite-fault inversions using seismic and high-rate GPS data, we have perturbed models to simultaneously provide slightly improved fits to near-field tsunami observations. The difference in information content and modeling approximations motivate parameter search approaches rather than joint inversion, both because the searches characterize the trade-offs and sensitivity to parameters and because weighting of the distinct information types is problematic for inversion. While the optimization is somewhat subjective as a result, insights are gained with regard to how the solutions behave. We find that 5–10° reductions of average fault strike, slight steepening of average fault dip and

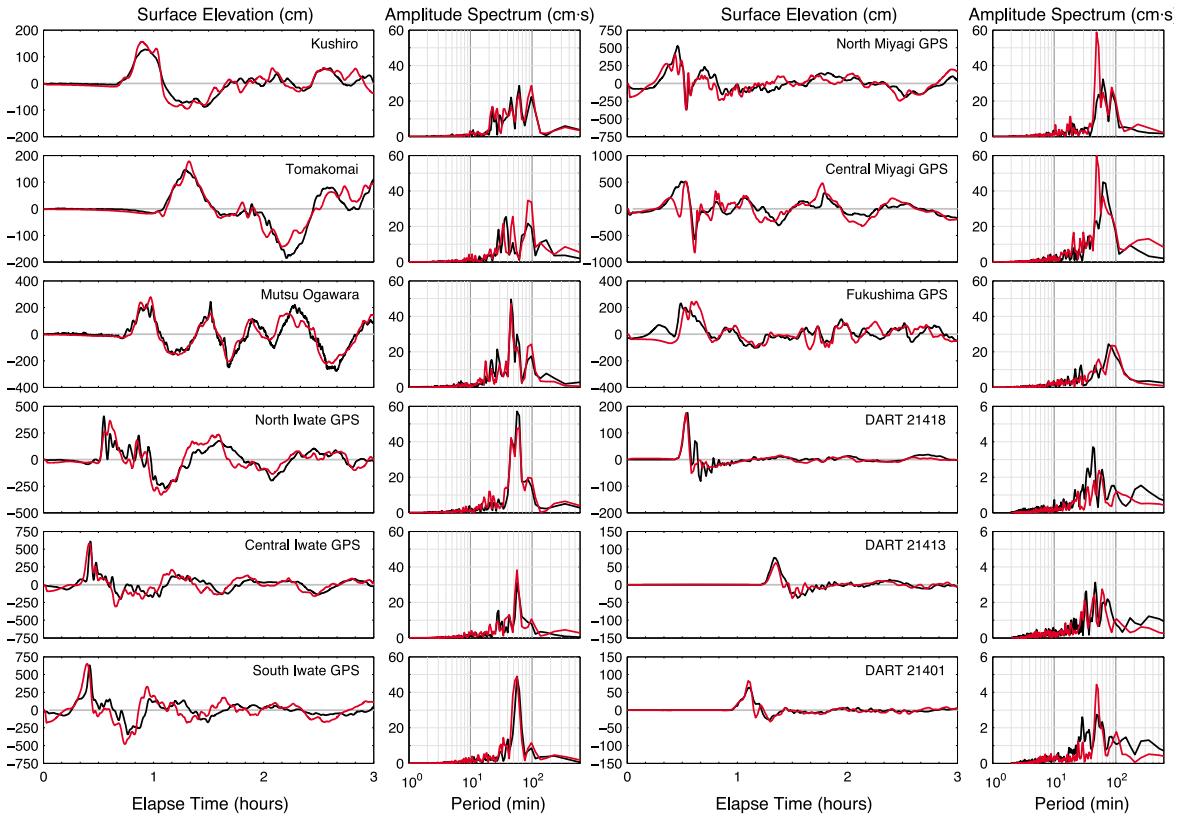

Figure 4. Comparisons of the observed (black lines) and the computed (red lines) time series and spectra of surface elevations at water level stations near Japan for preferred P-MOD3 ($\varphi_f = 192°$, $\delta = 12°$, $h = 22.5$ km).

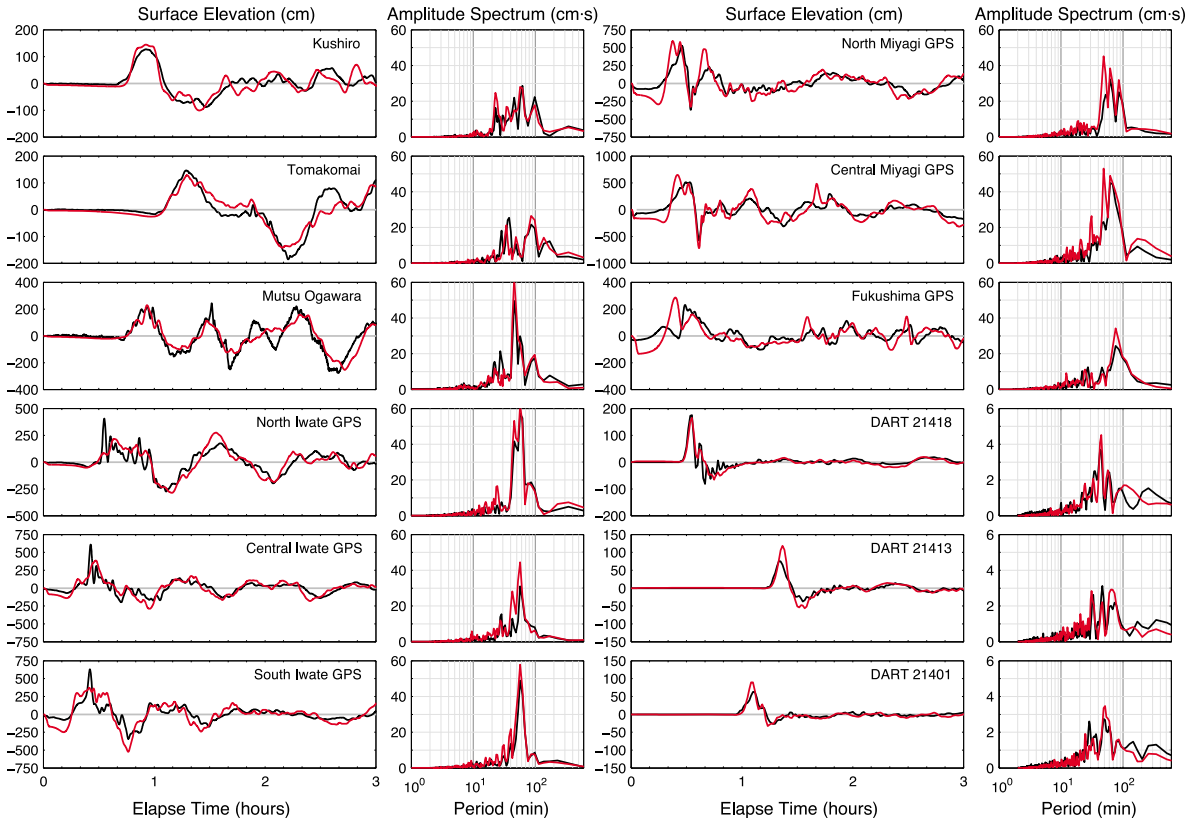

Figure 5. Comparisons of observed (black lines) and computed (red lines) time series and spectra of surface elevations at water level stations near Japan for hrGPS-2.

slight reduction of smoothing or increase of bandwidth improve simultaneous fits of the P wave, hr-GPS and near-field tsunami observations. The small changes in models can affect far-field tsunami observations as well, and if run-up calculations can be made more reliable, further progress toward unified models can be pursued with a combination of inversion and model search approaches.

[13] **Acknowledgments.** This work made use of GMT, SAC and Matlab software. The IRIS DMS data center was used to access the seismic data. We thank L. Rivera for providing the normal mode data set. Our hrGPS data, generously made available by C. Rocken of GPS Solutions, Inc. originated with efforts by GSI, NGDS, Hitz, GPSS, and VERIPOS. We thank T. Kuwayama for supplying the 20 arc-sec Japan bathymetry data. The recorded DART buoy data were obtained from the NOAA National Data Buoy Center. NOWPHAS GPS and wave gauges data maintained by Ports and Harbors Bureau, Ministry of Land, Infrastructure, Transport, and Tourism (MLIT), Japan, were provided by Port and Airport Research Institute (PARI), Japan. We thank the two anonymous reviewers for their thoughtful comments that have improved this paper. This work was supported in part by NSF grant EAR0635570 (T. L.). SOEST contribution 8492.

[14] The Editor thanks two anonymous reviewers for their assistance in evaluating this paper.

References

Ammon, C. J., T. Lay, H. Kanamori, and M. Cleveland (2011), A rupture model of the great 2011 off the Pacific coast of Tohoku earthquake, *Earth Planets Space*, *63*, 693–696, doi:10.5047/eps.2011.05.015.

Fujii, Y., K. Satake, S. Sakai, M. Shinohara, and T. Kanazawa (2011), Tsunami source of the 2011 off the Pacific coast of Tohoku earthquake, *Earth Planets Space*, *63*, 815–820, doi:10.5047/eps.2011.06.010.

Hayashi, Y., H. Tsushima, K. Hirata, K. Kimura, and K. Maeda (2011), Tsunami source area of the 2011 of the Pacific coast of Tohoku earthquake determined from tsunami arrival times at offshore observation stations, *Earth Planets Space*, *63*, 809–813, doi:10.5047/eps.2011.06.042.

Hayes, G. (2011), Rapid source characterization of the 2011 M_w 9.0 off the Pacific coast of Tohoku earthquake, *Earth Planets Space*, *63*, 529–534, doi:10.5047/eps.2011.05.012.

Ide, S., A. Baltay, and G. C. Beroza (2011), Shallow dynamic overshoot and energetic deep rupture in the 2011 M_w Tohoku-Oki earthquake, *Science*, *332*, 1426–1429, doi:10.1126/science.1207020.

Iinuma, T., M. Ohzono, Y. Ohta, and S. Miura (2011), Coseismic slip distribution of the 2011 off the Pacific coast of Tohoku earthquake (M9.0) estimated based on GPS data—Was the asperity in Miyagi-oki ruptured?, *Earth Planets Space*, *63*, 643–648, doi:10.5047/eps.2011.06.013.

Ito, T., K. Ozawa, T. Watanabe, and T. Sagiya (2011), Slip distribution of the 2011 off the Pacific coast of Tohoku earthquake inferred from geodetic data, *Earth Planets Space*, *63*, 627–630, doi:10.5047/eps.2011.06.023.

Koper, K. D., A. R. Hutko, T. Lay, C. J. Ammon, and H. Kanamori (2011), Frequency-dependent rupture process of the 11 March 2011 M_w 9.0 Tohoku earthquake: Comparison of short-period *P* wave backprojection images and broadband seismic rupture models, *Earth Planets Space*, *63*, 599–602, doi:10.5047/eps.2011.05.026.

Lay, T., Y. Yamazaki, C. J. Ammon, K. F. Cheung, and H. Kanamori (2011a), The 2001 Mw 9.0 off the Pacific coast of Tohoku earthquake: Comparison of deep-water tsunami signals with finite-fault rupture model predictions, *Earth Planets Space*, *63*, 797–801, doi:10.5047/eps.2011.05.030.

Lay, T., C. J. Ammon, H. Kanamori, L. Xue, and M. J. Kim (2011b), Possible large near-trench slip during the great 2011 Tohoku (M_w 9.0) earthquake, *Earth Planets Space*, *63*, 687–692, doi:10.5047/eps.2011.05.033.

Maeda, T., T. Furumura, S. Sakai, and M. Shinohara (2011), Significant tsunami observed at ocean-bottom pressure gauges during the 2011 off the Pacific coast of Tohoku earthquake, *Earth Planets Space*, *63*, 803–808, doi:10.5047/eps.2011.06.005.

Okada, Y. (1985), Surface deformation due to shear and tensile faults in a half space, *Bull. Seismol. Soc. Am.*, *75*(4), 1135–1154.

Ozawa, S., T. Nishimura, H. Suito, T. Kobayahi, M. Tobita, and T. Imakiire (2011), Coseismic and postseismic slip of the 2011 magnitude-9 Tohoku-oki earthquake, *Nature*, *475*, 373–376, doi:10.1038/nature10227.

Shao, G., X. Li, C. Ji, and T. Maeda (2011), Focal mechanism and slip history of 2011 Mw 9.1 off the Pacific coast of Tohoku earthquake, constrained with teleseismic body and surface waves, *Earth Planets Space*, *63*, 553–557, doi:10.5047/eps.2011.06.028.

Simons, M., et al. (2011), The 2011 magnitude 9.0 Tohoku-oki earthquake: Mosaicking the megathrust from seconds to centuries, *Science*, *332*, 1421–1425, doi:10.1126/science.1206731.

Yamazaki, Y., Z. Kowalik, and K. F. Cheung (2009), Depth-integrated, non-hydrostatic model for wave breaking and run-up, *Int. J. Numer. Methods Fluids*, *61*(5), 473–497, doi:10.1002/fld.1952.

Yamazaki, Y., K. F. Cheung, and Z. Kowalik (2011), Depth-integrated, non-hydrostatic model with grid nesting for tsunami generation, propagation, and run-up, *Int. J. Numer. Methods Fluids*, doi:10.1002/fld.2485, in press.

Yoshida, Y., H. Ueno, D. Muto, and S. Aoki (2011), Source process of the 2011 off the Pacific coast of Tohoku earthquake with the combination of teleseismic and strong motion data, *Earth Planets Space*, *63*, 565–569, doi:10.5047/eps.2011.05.011.

Yue, H., and T. Lay (2011), Inversion of high-rate (1 sps) GPS data for rupture process of the 11 March 2011 Tohoku earthquake (M_w 9.1), *Geophys. Res. Lett.*, *38*, L00G09, doi:10.1029/2011GL048700.

Zhao, D., Z. Huang, N. Umino, A. Hasegawa, and H. Kanamori (2011), Structural heterogeneity in the megathrust zone and mechanism of the 2011 Tohoku-oki earthquake (M_w 9.0), *Geophys. Res. Lett.*, *38*, L17308, doi:10.1029/2011GL048408.

K. F. Cheung and Y. Yamazaki, Department of Ocean and Resource Engineering, University of Hawaii at Manoa, Honolulu, HI 96822, USA.

H. Kanamori, Seismological Laboratory, California Institute of Technology, Pasadena, CA 91125, USA.

T. Lay and H. Yue, Department of Earth and Planetary Sciences, University of California, Santa Cruz, CA 95064, USA. (tlay@ucsc.edu)